Dextran-Based Nanoparticles to Formulate pH-Responsive Pickering Emulsions: A Fully Degradable Vector at a Day Scale

Valentin Maingret, Clémence Courrégelongue, Véronique Schmitt, Valérie Héroguez

Dextran-Based Nanoparticles to Formulate pH-Responsive Pickering Emulsions: A Fully Degradable Vector at a Day Scale

Valentin Maingret [a,b], Clémence Courrégelongue [a,b], Véronique Schmitt [a,*], Valérie Héroguez [b,*]

[a] Centre de Recherche Paul Pascal, UMR 5031 Univ. Bordeaux CNRS, 115 avenue du Dr Albert Schweitzer, 33600 Pessac, France.

[b] Laboratoire de Chimie des Polymères Organiques, Univ. Bordeaux, CNRS, Bordeaux INP, UMR 5629, Bordeaux, 16 Avenue Pey-Berland, F-33607 Pessac, France.

*corresponding authors
veronique.schmitt@crpp.cnrs.fr
heroguez@enscbp.fr

Abstract

Biosourced Pickering emulsion stabilizers with stimuli responsiveness are mostly designed for recycling and do not offer fast degradability as required for drug-delivery applications. Herein, dextran – a hydrophilic and biofriendly polysaccharide obtainable from biomass recovery – was used for the first time as a brick material for the formulation of (bio)degradable pH-sensitive Pickering emulsions. It was first modified with hydrophobic acetals moieties to provide pH-sensitive acetalated dextran. Under acidic conditions, it degrades into three biocompatible (macro)molecules: dextran, ethanol and acetone. Nanoparticles of acetalated-dextran were obtained using the nanoprecipitation process and could be similarly fully hydrolyzed under acidic conditions within 6 h. Then, O/W Pickering emulsions of dodecane (model oil) and medium-chain triglyceride (biocompatible oil) were successfully stabilized using these nanoparticles. pH-induced destabilization of these Pickering emulsions (including nanoparticles degradation) took less than 24 h. Finally, neither accumulation of nanoparticles nor harmful components release happened during the process, making this stimuli-responsive vector safe and environmentally friendly.

Keywords

modified polysaccharide, stimuli-responsive, Pickering emulsions, bio-friendly vector, biocompatible systems, nanoprecipitation.

1. Introduction

As surprising as it can be, mixing what is nonmiscible is at stake for a tremendous range of technologies. Emulsions enable to disperse one phase in another one, the two phases being nonmiscible. However, stabilizers must be introduced in the final formulation to ensure processability and kinetic stability. Surfactants are widely used to fill this purpose but present major drawbacks such as environmental toxicity and low stability efficiency[1].

Consequently, one can see the re-emergence of Pickering emulsions, observed more than a century ago by Walter Ramsden in 1903[2] and by Spencer Umfreville Pickering in 1907[3]. Instead of molecular surfactants, particles (ranging from dozens of nanometers to micrometers) are introduced and allow steric stabilization of the interfaces. This kind of emulsion is more stable owing to the much higher absorption energy[4] of particles compared to surfactants and does not need a lot of stabilizing material to achieve it, reducing toxicity.

Specifically, stimuli-responsive Pickering emulsions are of growing interest (from 0 to almost 60 papers/year in the last fifteen years, trend - rates estimated from Scopus) as they offer new possibilities for various applications (medicine, cosmetics, agriculture and food)[5–8]. They benefit from a high kinetic stability because of the particles anchoring at the droplets interface and can be destabilized on demand under a stimulus (pH, temperature, specific reagent, light and magnetic field[9–13]). Thus, if active compounds are encapsulated in the dispersed phase, they become available for the target. Responsiveness of this kind of system mainly relies on a change of affinity of the particles, allowing them to desorb thus leading to emulsion destabilization. To address the growing needs of environment friendly materials, biosourced nanoparticles (CNC and starch) have been used to stabilize pH-responsive Pickering emulsions[14–17]. No matter the strategy used to obtain pH-sensitivity[15] (leading to their desorption), (bio)degradation of these nanoparticles cannot be achieved by the stimulus itself and thus would require very specific conditions and long delay. This is useful for recyclability, but it may become an issue for drug-delivery-like applications because of their

potential accumulation and the unknown effects associated. One can note that chitosan is readily sensitive to pH as it can undergo a sol-gel reversible transition[18,19] but requires sharp control over pH to be implemented and lacks kinetic tunability. Thus, to the best of our knowledge, no study has ever considered Pickering emulsion stabilizers which could be fully degraded at a short time scale (day/week) using only pH stimulus to do so.

In this respect, we developed new pH-responsive Pickering emulsions with (bio)degradable and bio-sourced nanoparticles based on dextran. This system offers long time stability for storage but can be destabilized within a day under acidic conditions, because of the hydrolysis of the stabilizing nanoparticles. Degradation of the stabilizers and emulsion destabilization are then coupled because the obtained (macro)molecular products can no longer stabilize the emulsion. Above all, these products are biodegradable and of no consequence for the environment. Consequently, no nanoparticles can accumulate, and all the produced materials are completely safe, making this new class of stimuli-responsive Pickering emulsion stabilizers suitable for drug-delivery-like applications. The raw material used to design such nanoparticles is dextran, a biosourced, biodegradable and biocompatible hydrophilic polysaccharide[20]. It is a by-product of the sugar industry and it can be obtained from food wastes, promoting biomass recovery[21]. It is then cheap and obtainable from renewable resources.

In the present paper, dextran was modified to produce acetalated dextran (Ace-dextran)[22]. This modification can be undone under aqueous mild acidic conditions (pH 4.8), generating three biocompatible products: dextran, acetone and ethanol. Using this material, nanoprecipitation was performed to obtain for the first time Ace-dextran nanoparticles. We then successfully formulated direct Pickering emulsions and observed the typical limited coalescence phenomenon[23]. In the current literature, the use of dextran to produce Pickering emulsion stabilizers is limited to the formation of conjugate microgels[24]. Thus, this is the first attempt to use dextran-only-based nanoparticles as Pickering emulsions stabilizers. Finally, we proceeded with some destabilization attempts: first on nanoparticles alone and then on the nanoparticle-stabilized emulsions. Nanoparticles are fully

hydrolyzed under acidic conditions, releasing simple and biocompatible materials: dextran, ethanol and acetone. As a consequence of the nanoparticle degradation, the emulsions could also be destabilized, with a slower kinetics.

2. Experimental Section

2.1 Materials

Dextran (M_w=40 000 g/mol, M_n=26 000 g/mol, Đ=1.3 as measured by the authors using Size Exclusion Chromatography) and 2-ethoxypropene (95%) were purchased from ABCR. Anhydrous dimethyl sulfoxide (DMSO, ≥99,9%) and dodecane (99%) were purchased from Sigma-Aldrich. Triethylamine (TEA, 99%) was purchased from Fisher Scientific. Pyridinium-*p*-toluenesulfonate (PPTS, 98%) was purchased from Fluka. Medium-chain triglyceride (MCT) "Miglyol 812N" was furnished by Stéarinerie Dubois.

All reagents were used with no further purification unless noted. Solvents used are of analytical grade.

2.2 Dextran modification to yield Acetalated-dextran (Ace-dextran)

The dextran modification was adapted from the work of Kauffman et al. [22]. Typically, lyophilized dextran (6.17 mmol relative to glucosidic units, 1 g) and PPTS (0.0617 mmol, 15.5 mg) catalyst were dissolved into anhydrous DMSO (10 mL) before reaction with 2-ethoxypropene (37 mmol, 3.19 g) under nitrogen gas (Figure 1) at 20°C. The reaction was quenched with 1 mL of TEA after 50 min and reaction medium was then precipitated in basic water (pH 9, 0.02% v/v TEA/water), vacuum filtered and lyophilized. The solid was then solubilized in absolute ethanol and centrifuged (10 min at 11 000 rpm). Finally, the supernatant was precipitated in basic water (pH 9, 0.02% v/v TEA/water), vacuum filtered and lyophilized to yield a white fluffy powder.

To characterize the final product, a suspension of Ace-dextran in D_2O (10 mg in 0.9 mL) was prepared and 0.1 mL of D_2SO_4 was added to induce hydrolysis. A ^1H nuclear magnetic resonance (^1H NMR) spectrum was recorded using a 400 MHz NMR instrument (Bruker 400 Ultra Shield) (Figure S1). Three important peaks are then used to determine the modification rates: ethanol (produced from the hydrolysis of an acyclic acetal), acetone (produced from the hydrolysis of a cyclic and an acyclic acetal) and two hydrogens from dextran. Finally, peak integrations of acetone and ethanol can be standardized for each glucose unit as described by Kauffman et al. [22] and alternatively by Bachelder et al. [25] to calculate the acyclic and cyclic modification ratios (Supporting Information SI.2). The overall modification rate represents the number of substituted hydroxyl groups per 100 glucosidic units.

Two syntheses with the same experimental conditions were carried out, they will be called S1 and S2 for clarity purpose and their characteristics are given in the Results and Discussion section.

2.3 Nanoprecipitation of Ace-dextran

Nanoparticles were produced through nanoprecipitation using a syringe pump (CHEMYX Fusion 101 Syringe Pump). Specifically, Ace-dextran was dissolved in tetrahydrofuran (THF) (5 g/L) and injected in a 40 mL water bath at 0.4mL/min. At the end of this process, an additional 40 mL of water was added to the dispersion, making an osmotic shock in the case of remaining good solvent into aggregates. After concentration, the dispersion of nanoparticles was centrifuged (20 min at 11 000 rpm). The supernatant was discarded, and the nanoparticles were dispersed with basic water (pH 9, 0.02% v/v triethylamine/water) to prevent any early degradation. Nanoparticles were centrifuged three times following the same process to eliminate potential residual free chains. Finally, the recovered dispersion was concentrated using a rotary evaporator (40 °C bath) to eliminate water. The concentrated dispersion can be stored several months without stability issues.

Two different nanoparticle dispersions were produced. They will be named NPDx, where x stands for the synthesis number of the Ace-dextran used for nanoprecipitation. Therefore, products from S1 and S2 were used to produce NPD1 and NPD2.

The mass concentration of nanoparticles into dispersions was determined using the residual dry weight technique.

Shape characterization of the nanoparticles was done by transmission electron microscopy (TEM) on a HITACHI H-600 instrument (HV =75 kV). From TEM pictures and using ImageJ software, size measurements of at least 100 nanoparticles were obtained, the volume-averaged diameter D[4,3] of nanoparticles was calculated following eq. 1:

$$D[4,3] = \frac{\sum_i^n d_i^4}{\sum_i^n d_i^3} \quad (1)$$

where d_i is the diameter of a nanoparticle from an *n*-nanoparticles population.

The size distribution of the nanoparticles and their average diameter (z in nm) were characterized by dynamic light scattering (DLS) using a NanoZS90 instrument (Malvern Instrument Ltd, UK). The wavelength used was 630 nm and the scattering angle set to 90°. The temperature was kept at 25 °C unless noted. Systematically, three measurements of 10 runs (30 s each) were taken to ensure data reliability. The concentration of the sample was low enough to avoid multiple scattering and is given when necessary. Size distribution is characterized by an average diameter (z, in nm) and a typical standard deviation (σ, in nm) or by the polydispersity index (PDI) calculated as follows eq. 2:

$$PDI = \left(\frac{\sigma}{z}\right)^2 \quad (2)$$

Multi angle light scattering (MALS) measurements were performed using an ALV-5000 goniometer with a He-Ne laser (633nm) and an ALV-5000/EPP multiple τ digital correlator (initial sampling time

of 125 ns). For static scattering six measurements of 5 s each were proceeded with an angle step of 5 ° from 50 ° to 150 °. The temperature of the toluene bath was kept to 20°C. Five samples with decreasing concentrations were characterized (from 0.08 g/L to 0.008 g/L). Data acquired on ALV correlator software were used to calculate the radius of gyration (R_g) and the molar mass of the nanoparticles (Mw) using a Guinier Plot. Full calculations and methods are provided in the Supporting information (SI.3,4,5,8,9 and Figure S6, S7 and S10).

Swelling of the nanoparticles was quantified by comparison of the average polymer density in the nanoparticle (determined by MALS) to the density of free chains of similarly modified dextran at dry state (1.37, determined by pycnometry). The proportion of absorbed water ($\%m_{water}$) with respect to a nanoparticle dry mass (m_D) was defined as follows eq. 3: [26]

$$\%m_{water} = \frac{m_w}{m_D} \quad (3)$$

Considering that the mass of a dry nanoparticle is equal to the mass of the polymer it contains and hypothesizing ideal mixing, the previous relation can also be written as eq. 4:

$$\%m_{water} = \frac{(V_S - V_D) * \rho_{water}}{V_S * \rho} \quad (4)$$

where V_S and V_D are the volumes of the nanoparticle in its swollen and dry state respectively and ρ is the average polymer density in the swollen nanoparticle. Because of polymer mass preservation $m_{polym} = m_D = V_S * \rho$. The geometrical radius from MALS measurements (median value between R_h and R_g) was chosen to calculate V_S.

The water mass fraction content of a swollen nanoparticle can be then expressed as follows (eq. 5):

$$\Phi_w^m = \frac{\%m_{water}}{1 + \%m_{water}} \quad (5)$$

2.4 Formulation of Pickering emulsions

Emulsions were formulated using a water phase / oil phase (dodecane or MCT) ratio of 50/50 or 80/20 v/v with the total liquid volume set to 4 mL. A calculated amount of nanoparticle dispersion was diluted into the pure aqueous phase to obtain the target concentration. Then the oil was added, and the biphasic solution was stirred using an Ultra Turrax (IKA T25) at 20 000 rpm for 2 min with a shaft (S25N 10G). Nanoparticles quantity is noted here as a concentration relative to the volume of dispersed phase. As only O/W emulsions were formulated in this work, nanoparticle concentration was related to the volume of oil (despite nanoparticles being unable to disperse in the oil phase). This is meaningful because the volume of oil and the drop size define the total interfacial area to be covered by the nanoparticles.

The water phase/oil phase ratio was set to 50/50 v/v to assess the kind of emulsion stabilized by the nanoparticles (O/W or W/O). Once prepared, a small amount of the emulsion was taken and put in two different vials containing water and oil, respectively. In the case of an O/W emulsion, the aliquots dilute easily into water, not in oil. This is the reverse case considering W/O emulsions.

The emulsions were observed with an optical microscope (Zeiss Axioskop 40) in bright field using x5 and x10 objectives. Pictures of the emulsions and of metric scales were taken using a digital camera device linked to the microscope. From these, using the image treatment software ImageJ, size measurements of at least 200 drops were obtained.

To describe the mean drop size of the emulsions, the Sauter diameter (eq. 6) was used:

$$D[3,2] = \frac{\sum_i^n d_i^3}{\sum_i^n d_i^2} \qquad (6)$$

where d_i is the diameter of a drop from an *n*-drops population. The Sauter diameter is defined as the surface-average diameter of the drops. Finally, to describe the drop size distribution width of the emulsions, a typical standard deviation was calculated following (eq. 7):

$$S = \sqrt{\frac{\sum_i^n (d_i - D[3,2])^2}{n}} \quad (7)$$

Cryo-SEM was performed on emulsion droplets to check the presence of nanoparticles at the interface. A dodecane-in-water emulsion was formulated with the concentration of nanoparticles set to 6 mg/mL of oil. The sample was observed without the use of a replica.

2.5 pH-induced degradation of Ace-dextran nanoparticles

A small amount of the nanoparticle dispersion was put in a DLS cuvette filled with freshly made acetic buffer (pH 4.8) to obtain a slightly bluish dilute dispersion. The concentrations of nanoparticles were set equal to 0.04, 0.08 and 0.16 mg/mL to determine the influence of concentration on the degradation kinetics.

DLS analysis was immediately conducted after nanoparticles went in contact with the buffer. The DLS cuvette was heated at 37 °C, which is the working temperature for many biological systems including the human body. One measurement of 10 runs of 30 s was proceeded every 10 min during a total time of almost 6 h.

From a DLS measurement, one can obtain the raw signal of the scattered signal named derived count rate (DCR) in kilocounts per seconds (kcps). This signal intensity is directly related to the concentration of diffusive entities in the sample (i.e., the nanoparticle concentration c_p) and their size (z) (eq. 8) [27]:

$$DCR \propto c_p * z^6 \quad (8)$$

Both size and DCR were measured during the degradation. As the size of the nanoparticles did not change, DCR was directly proportional to the concentration of nanoparticles (calibration curve of DCR with various concentrations can be found in Figure S11). Thus, collecting the DCR data as a function of time and normalizing them by the first obtained value allowed quantifying the nanoparticles and therefore reporting their degradation [27].

2.6 pH-induced destabilization of formulated Pickering emulsions

The same freshly made acetic buffer (pH 4.8) as for the degradation of nanoparticles was used. Emulsions with a water phase / oil phase ratio of 80/20 v/v and a nanoparticle concentration of 6 mg/mL relative to the dispersed phase were prepared under the same conditions as described before. For testing the emulsion destabilization, 2 mL of acidic buffer was added whereas 2 mL (the same volume) of water was added in the control sample. Then both samples were kept at 37 °C on a shaker plate at 50 rpm. Pictures of the emulsion cream were taken at regular time intervals to monitor emulsion stability. Moreover, tiny aliquots of the emulsion cream were withdrawn to observe the microscopic structure over time. We checked that this operation did not affect emulsion stability.

3. Results and discussion

3.1. Dextran modification to yield Acetalated-dextran (Ace-dextran)

Ace-dextran was prepared following the reaction scheme in Figure 1 at 20 °C. This dextran modification led to the replacement of some hydroxyl groups of the glucosidic units by acetals which can be either cyclic or acyclic. The number of acetals and their nature (cyclic or acyclic) were determined by performing ^{1}H NMR on the totally hydrolyzed Ace-dextran.

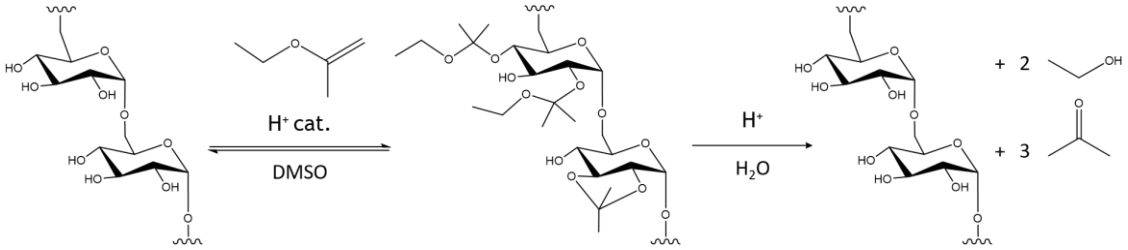

Figure 1. Reaction scheme for the formation of Ace-dextran with 2-ethoxypropene and its degradation in aqueous acidic medium

Table 1. Grafting Rates Determined by ^{1}H NMR

Synthesis	S1	S2	Kauffman et al. [22]
Cyclic acetal rate	0.57	0.61	0.64
Acyclic acetal rate	0.98	1	0.99
Overall modification	213 %	223 %	227 %
Reaction temperature	20°C	20°C	Room Temp.

During hydrolysis, a cyclic acetal is cleaved into an acetone molecule whereas an acyclic acetal is cleaved into an acetone and an ethanol molecule (Figure 1). By integrating methyl protons of acetone (B, δ=2.2 ppm Figure S1) and ethanol (C, δ=1.1 ppm Figure S1) and normalizing them by the C_6

hydrogens from the dextran glucosidic unit (A, δ=3.9 ppm Figure S1) one can determine the relative grafting rate of cyclic and acyclic acetal onto dextran (Supporting Information SI.2).

Two batches of Ace-dextran were synthesized and then characterized by ^{1}H NMR after hydrolysis (Supporting Information SI.2). Cyclic and acyclic acetal grafting rates obtained are summarized in Table 1, and calculations are described in (Supporting Information SI.2).

3.2. Nanoprecipitation of Ace-dextran

3.2.1 Nanoparticle Synthesis

Ace-dextran nanoparticles were prepared through nanoprecipitation. This process has been extensively used for the preparation of nanoparticles [28,29], including modified dextran-based ones [30–32]. However, it is the first that time Ace-dextran (modified with ethoxypropene) nanoparticles are obtained with this method. Kauffman et al. [22] used the emulsion/evaporation process to produce microparticles. Using this process, they had to introduce PVA (polyvinyl alcohol) chains to stabilize the emulsion, which may remain in the final dispersion. As our goal is to use the particles to stabilize emulsions, this could lead to biased results. Thus, as nanoprecipitation was done with no additional stabilizer, the nanoparticle dispersion obtained was composed of only Ace-dextran. In addition, the minimum size of Pickering emulsions droplets is intrinsically related to the size of the particles anchored at the surface. Starting from microparticles would have shorten the field of possibilities. Ace-dextran was solubilized in a good solvent and then added dropwise in an anti-solvent bath solution (miscible with the good solvent). As the good solvent diffuses into the anti-solvent bath, polymer chains start to collapse and associate to form spherical aggregates to yield nanoparticles whose size is governed by the process parameters. The solvent used to solubilize Ace-dextran was THF because it diffuses well in water and is easily removable by evaporation. This nanoprecipitation

process is in accordance with the requirements of green engineering and manufacturing as it avoids the use of large quantities of energy and solvent.

3.2.2. Nanoparticle characterizations

TEM characterizations were performed on NPD1 nanoparticles to determine their shape. As shown on Figure 2, the nanoparticles are spherical - making the following DLS measurements reliable - and well defined. In addition, we were able to assess their size and found out a D[4,3] of 122 ± 35 nm.

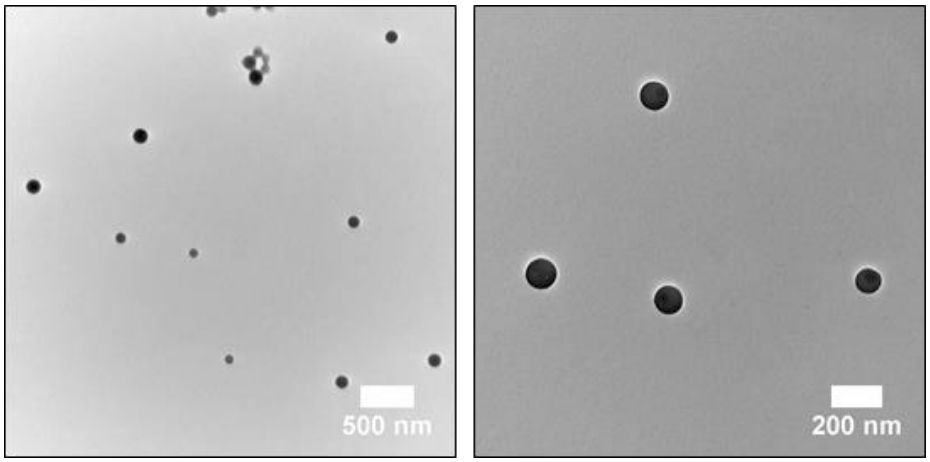

Figure 2. TEM images of nanoparticles from NPD1

According to DLS measurements, narrow size distribution of nanoparticles with an average hydrodynamic diameter of around 200 nm was obtained (Table 2). The higher value obtained for NPD1 nanoparticles (compared to TEM results) may be due to the different state of the nanoparticles (in water vs dried under vacuum) and probably indicates that a swelling is occurring. This will be discussed at the end of this part.

Table 2. Size distribution measurements obtained of NPD1 and NPD2 by DLS 90° and TEM

NPD (Measurement)	NPD1 (TEM)	NPD1 (DLS 90°)	NPD2 (DLS 90°)
Average diameter z (nm)	122 ± 35	220 ± 71	229 ± 61
PDI	0.08	0.105	0.072

To check the repeatability of the process, different nanoparticle batches starting from the same Ace-dextran synthesis were analyzed by DLS. All exhibited relatively the same size keeping a quite low PDI of 0.1 or below. This made possible to assemble different nanoprecipitation batches obtained from the same product without compromising narrow monomodal distribution.

Multi-angle static light scattering (SLS) was performed to calculate NPs gyration radius (R_g) and molar mass (M_w) in water (Supporting Information SI.5, Figure S6 and S7). From this, it was possible to calculate the average density of polymer in the nanoparticles (Supporting Information SI.8). The density of polymer in the particles will be required later in this work to calculate the coverage rate of the Pickering emulsion droplets by the nanoparticles. Results and relative standard deviations are given in Table 3.

Table 3. Multi angle SLS results using Guinier Plot and density calculation of the NPs from NPD1

R_g (nm)	M_w (g/mol)	ρ (g/mL)
89.64 (± 1.9 %)	$1.384\ 10^9$ (± 1.08 %)	0.685 (± 15 %)

From these results, the swelling of nanoparticles into water could be appreciated. Indeed, the polymer density decreased from 1.37 (free chains – dry state) to 0.685 in the nanoparticle, meaning that the volume of a nanoparticle in water is twice the one of a "dry" one. The radius of a "dry" nanoparticle would be then equal to 147 nm, which follows TEM measurements results (122 ± 35 nm). In order to quantify the swelling of nanoparticles by water, proportion of absorbed water ($\%m_{water}$) was computed

according to eq. 4 and was equal to 0.73, indicating that the water mass fraction Φ_w^m (eq. 5) of the nanoparticles is equal to 42%. Therefore, the nanoparticles are made of 42% weight of water and 58% of the polymer.

3.2.3. NP Stability

Water dispersions of nanoparticles were stored in a transparent vial (to check turbidity or sedimentation) protected from light during storage in a cupboard. No major destabilization phenomenon occurred in more than 10 months, except slight but reversible sedimentation. This was confirmed by size distribution measurements obtained by DLS at t_0 and $t_{10months}$ (Figure S12).

3.3. Formulation of pH-sensitive Pickering emulsions

3.3.1. Emulsion type

Emulsions of water phase/oil phase ratio 50/50 v/v were first formulated to assess the type of emulsion stabilized. O/W emulsions were formed. Dodecane emulsions all creamed quickly because of the large diameter of the droplets and the low density of dodecane (0.75 $g.cm^{-3}$) compared to water.

3.3.2. Influence of nanoparticle concentration - Limited coalescence phenomenon

O/W Pickering emulsions were formulated varying the amount of nanoparticles (expressed as a concentration of nanoparticles relative to the volume of the dispersed phase). We observed microscopically that the average diameter of the droplets decreased when adding more stabilizing material (low concentrations range). This phenomenon is typical of Pickering emulsions and is called limited coalescence [23]. Coalescence is in general a deleterious destabilization phenomenon but in this

366 case, one can take advantage of it - because it is limited - to produce narrow monomodal emulsions
367 [33] with great re-feasibility. During the emulsification process, a large excess of interfacial area is
368 produced compared to the area that can be covered by the stabilizing nanoparticles. Consequently,
369 drops which are not enough covered coalesce to decrease the interfacial area. As the stabilizing
370 particles are irreversibly anchored at the interface, the coalescence phenomenon stops when the drops
371 are covered enough.
372 In this context, it has been proven that the inverted Sauter diameter of the droplets is linearly related
373 to the amount of nanoparticles used to stabilize them, as described in eq. 9 [34]:

374 $$\frac{1}{D[3,2]} = \frac{c_p}{4C\rho_p d_p} \quad (9)$$

375 where c_p is the concentration of particles relative to the volume of the dispersed phase (oil – computed
376 from residual dry weight results), ρ_p is the particle density (here the average polymer density in the
377 nanoparticle ρ computed earlier), d_p is the geometrical particle diameter, and C is the surface coverage,
378 that is, the fraction of the droplet interfacial area covered by the particles. Using nanoparticles from
379 NDP1, we were able to observe this relationship for low concentrations, followed by a plateau (Figure
380 3). Detailed size measurements of Pickering emulsions are described in the Supporting Information
381 (Figure S13).

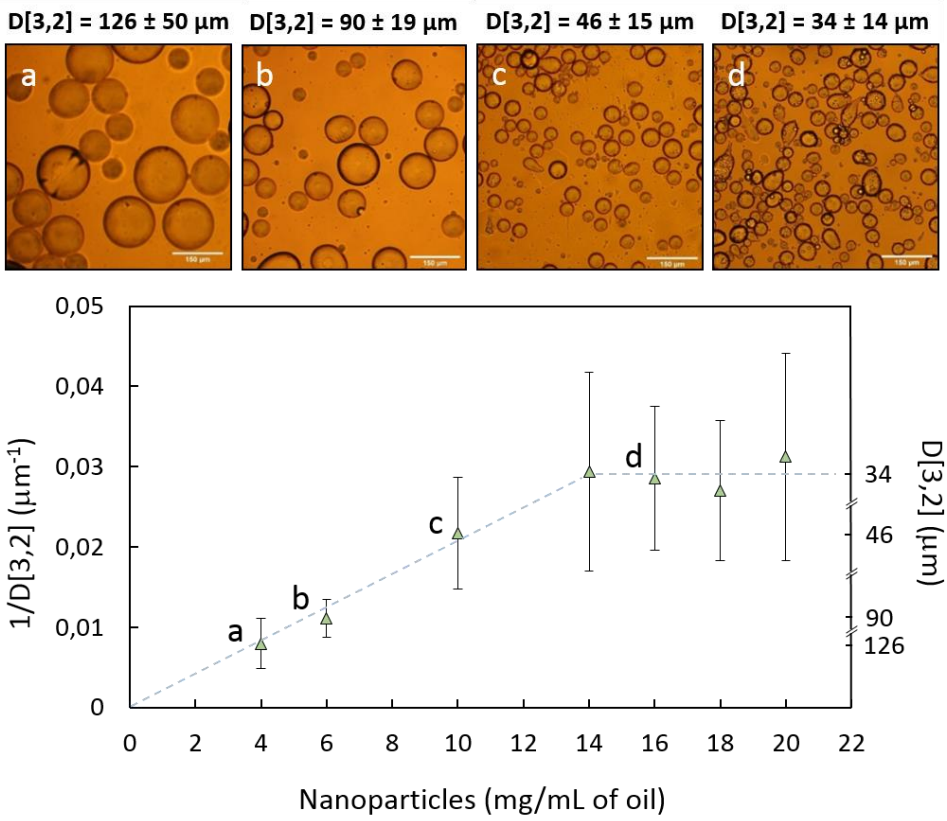

382

383 *Figure 3. Microscopic pictures of formulations with various concentrations: 4 mg/mL of oil (a), 6*
384 *mg/mL of oil (b), 10 mg/mL of oil (c), 16 mg/mL of oil (d) – scale bar is equal to 150 µm (top) -*
385 *Evolution of 1/D[3,2] as a linear function of the nanoparticle (from NPD1) concentration, followed*
386 *by a plateau (bottom)*

387 This linear relation is applicable for a range of low concentrations. At some point (beginning of the
388 observed plateau), there are enough nanoparticles to fully stabilize drops formed by stirring. Then,
389 no more coalescence can occur, and the drops diameter is set by the process (shearing source is
390 responsible for area creation). As a result, there is no coalescence and the final size of the droplets
391 will not change when adding more nanoparticles. Usually the emulsions, obtained out of the limited
392 coalescence domain, are polydisperse as their size distribution directly result from turbulent stirring.
393
394 From the slope of the linear domain of limited coalescence, one can obtain the surface coverage C of
395 the oil droplets. Density and geometrical diameter of the particle used were determined using MALS

396 data (Figure S7). As a result, the calculated coverage is of 0.94 ± 0.14 (Supporting Information SI.8
397 Figures S9 and S10) which is close to that of a hexagonally close-packed narrow monomodal particles
398 organization at 2D where C=0.9 [35].
399 Cryo-SEM experiments were performed to visualize the interface of dodecane-in-water emulsion
400 droplets. The concentration of nanoparticles used was 6 mg/mL (in the limited coalescence domain)
401 meaning that the coverage should be the same as the one calculated above. From the Cryo-SEM
402 picture (Figure 4), it can be deduced that the dodecane droplet is fully and densely covered with
403 nanoparticles. This is in good agreement with the coverage result deduced from optical microscopy
404 observations in the limited coalescence domain. Moreover, this close-packed organization may be
405 favored by the swelling state of the nanoparticles, probably making them softer and a little bit
406 deformable as they are composed of 42% of water. Thus, instead of spheres, it seems that some
407 polyhedrons can be distinguished on Figure 4. However, it is worth strengthening that swelling did
408 not induce nanoparticles sticking at the interfaces as no flocculation was observed.
409

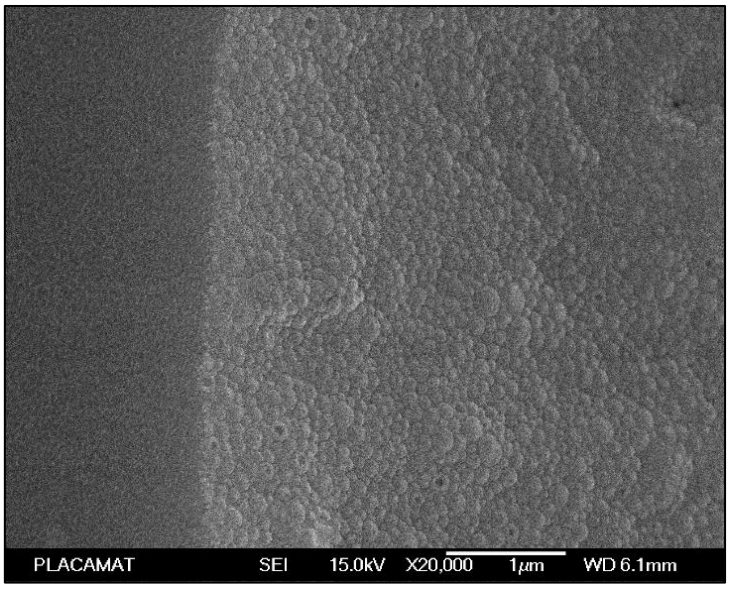

410

Figure 4. Cryo-SEM picture of the surface of a dodecane droplet in water stabilized by Ace-dextran nanoparticles (6 mg/mL of oil)

To summarize, nanoparticles of Ace-dextran can be used to formulate stable Pickering O/W emulsions in a controlled way as the amount of introduced nanoparticles defines the final diameter of the oil drops. The drops are densely covered by a monolayer of nanoparticles.

3.4. pH-induced destabilization of formulated Pickering emulsions

Assessment of the pH-induced destabilization of the formulated Pickering emulsions was done in two main steps. First, pH-induced degradation kinetics of Ace-dextran nanoparticles suspended in water was studied. Then, Pickering emulsions were subjected to the same acidic conditions to study the destabilization mechanism and kinetics.

3.4.1. pH-induced degradation of Ace-dextran nanoparticles

Ace-dextran is hydrolyzed in aqueous acid medium, producing three fully biocompatible and biodegradable products: dextran, ethanol and acetone. When assembled into nanoparticles the same mechanism occurs and these nanoprecipitates finally tend to be solubilized into the acidic water medium. DLS measurements of the nanoparticles from NPD1 in acidic medium were performed to study the degradation kinetics. The DCR signal value and nanoparticles average size were plotted against time of exposure to the pH 4.8 buffer (Figure 5). The obtained values were all normalized by the first one at t_0.

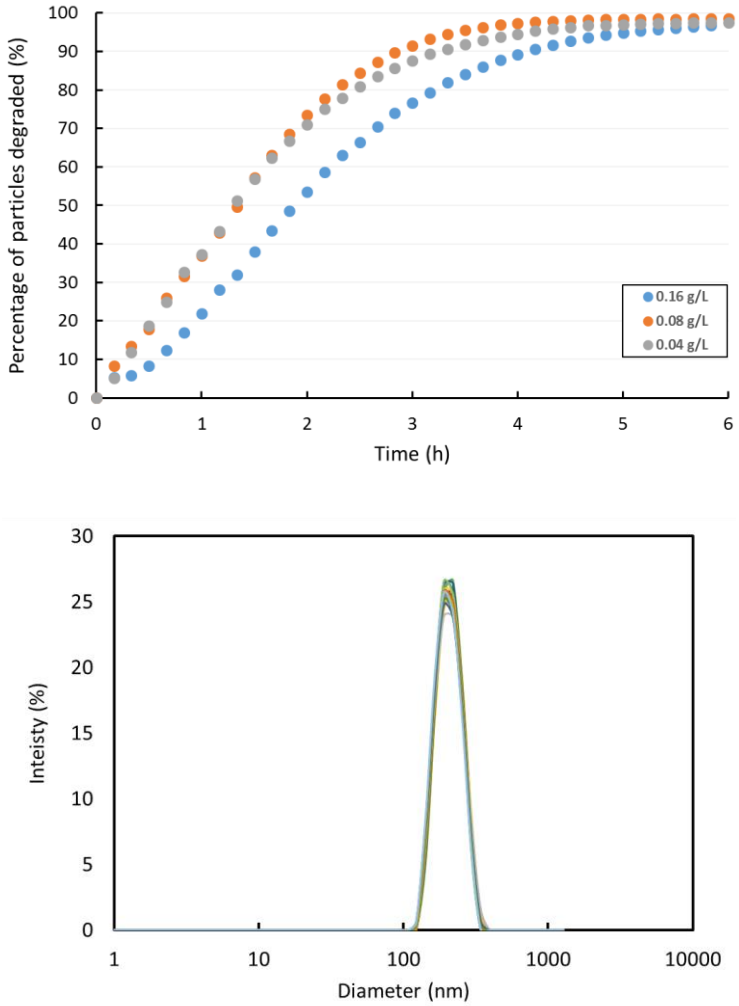

Figure 5. Degradation of nanoparticles over time under acidic conditions (pH 4.8 buffer) at various concentrations (top) and size distributions of nanoparticles from t_0 (0% of degradation) to t_{4h} (90% of degradation) with an initial concentration of 0.16g/L (bottom).

First, no variation in size measurements meant that DCR measurements were relevant because its value only depends on the number of nanoparticles in the system. We varied the concentration of nanoparticles to see if it would change the degradation kinetics. The nanoparticles' average size did not change drastically with time, whatever the used concentration. In addition, all size distributions superimpose showing that there is no time evolution of the distribution. From these, we can conclude that no erosion mechanism occurs, which is in accordance with the fact that nanoparticles are swollen in water. One can assume that the nanoparticle keeps its integrity until its chains become partially soluble in water at some critical point, leading to the total solubilization of the nanoparticle. Indeed,

no small aggregates resulting from the hydrolysis of the nanoparticle were detected. Kauffmann et al.[22] worked on the degradation of microparticles of Ace-dextran and explained that a more or less pronounced burst mechanism could be involved, depending on the ratio of acyclic acetals, which are hydrolyzed first. However, as the pH used for degradation and the particle scale are not the same here, it would not be relevant to directly compare the obtained results.

Nanoparticle concentration did have a slight influence on the degradation time (Figure 5 top), but with no clear trend as the 0.04 g/L sample took more time than the 0.08 g/L sample. The shape of this degradation curve is almost linear at the beginning except a small delay for the 0.16 g/L sample. Then the slope starts to decrease to finally reach a plateau (total degradation, limit of detection for DLS). The absence of stirring in the DLC cuvette during the measurements may have influenced the obtained profiles but allowed to follow the degradation in situ and in line.

Nanoparticle concentration used for the following Pickering emulsions is typically 6 mg/mL oil, corresponding to 1.5 mg/mL water that is almost 10 times more than the highest concentration used in this study (0.16 mg/mL). Making the same experiments at such a high concentration was not possible because of opacity incompatible with DLS measurements.

3.4.2. pH-induced destabilization of formulated Pickering emulsions

Formulated Pickering emulsions stabilized by nanoparticles from NPD1 (6 mg / mL of oil) were fully characterized and then ssubjected to pH-induced destabilization by injection of an acetic buffer at pH 4.8. Nanoparticles from this material were hydrolyzed in 6 h according to the previous part, assuming that the high concentration does not impact the degradation kinetics. Thus, emulsions stabilized with such nanoparticles were subjected to destabilization in acidic conditions because of the disappearance of their stabilizers. To better understand the involved mechanisms, both microscopic and macroscopic studies were performed during the destabilization process.

468

469 **3.4.2.1. Microscopic study**

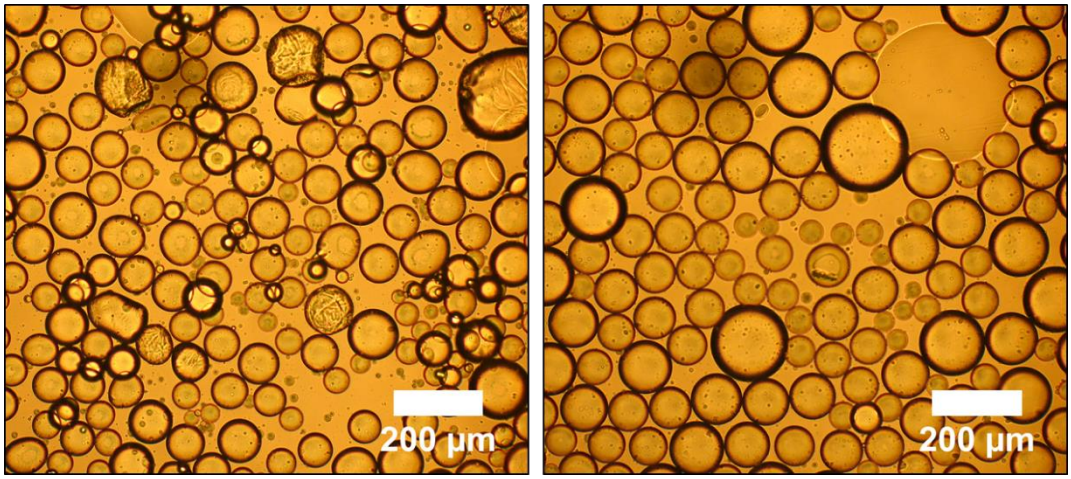

470

Figure 6. Optical microscope images before adding the acidic buffer (left) and 5 h after adding the acidic buffer (right)

471

472 Size measurements performed as shown in Figure 6 showed that the Sauter diameter increased from
473 75 µm to 110 µm in 5 h. In other words, considering the dispersed phase volume preservation, it
474 corresponds to the coalescence of three droplets on average during this time. Droplets showed only a
475 spherical shape and still a narrow monomodal distribution. From this, we can assume that the
476 coalescence process was quite homogeneous after 5 h. This microscopic effect and the final
477 macroscopic consequence (demixing) are due to a multi-scale succession of events (Figure 7). At the
478 molecular scale, acyclic and cyclic acetals are hydrolyzed continuously into acetone and ethanol
479 because of the aqueous acidic medium. Consequently, at the macromolecular scale the Ace-dextran
480 chains become more and more hydrophilic to a critical point where the whole nanoparticle can be
481 solubilized. Hydrolysis of nanoparticles leads to the decrease in the oil droplets coverage which was
482 rather high at the beginning (C=0.94). A coalescence event between two droplets provides an increase
483 in the coverage (26% for initially identically sized drops). To ensure shape relaxation of the new
484 formed droplet, its new coverage should be no more than 0.9. Thus, in the case of two identical
485 droplets, their respective coverage should be at least lower than 0.71. On the other side, coalescence

is happening until the coverage of the newly formed droplet is high enough (like the limited coalescence phenomenon occurring right after formulation). Hence, whereas the degradation of nanoparticles may be continuous, the emulsion destabilization process is intrinsically discontinuous. The coverage of a droplet increases right after coalescence but is also continuously decreases because of the hydrolysis of the nanoparticles, until another coalescence event (Figure 7). In the end, the size of the droplets becomes too high, leading to macroscopic leakages. Consequently, it is quite certain that not all the nanoparticles are hydrolyzed neither when the emulsion starts to be unstable nor when it is totally demixed. However, there is no doubt that they will be all hydrolyzed in the end as they become more and more available to the water phase that is the same conditions of the pH-induced degradation of the nanoparticles described earlier (total degradation in 6 h). This scenario is confirmed by the macroscopic observation.

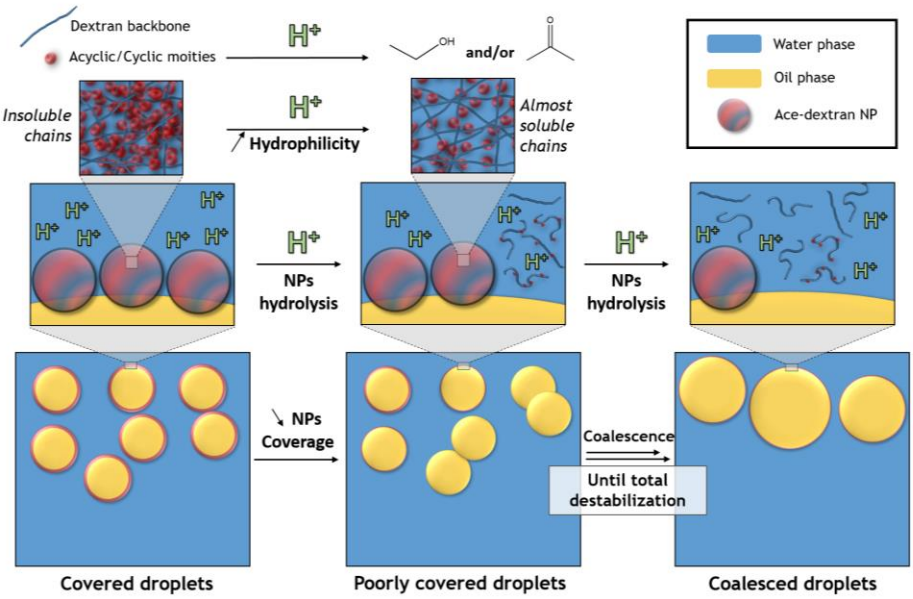

Figure 7. Multi-scale mechanism for the Pickering emulsion destabilization under acidic pH conditions

3.4.2.2. Macroscopic study

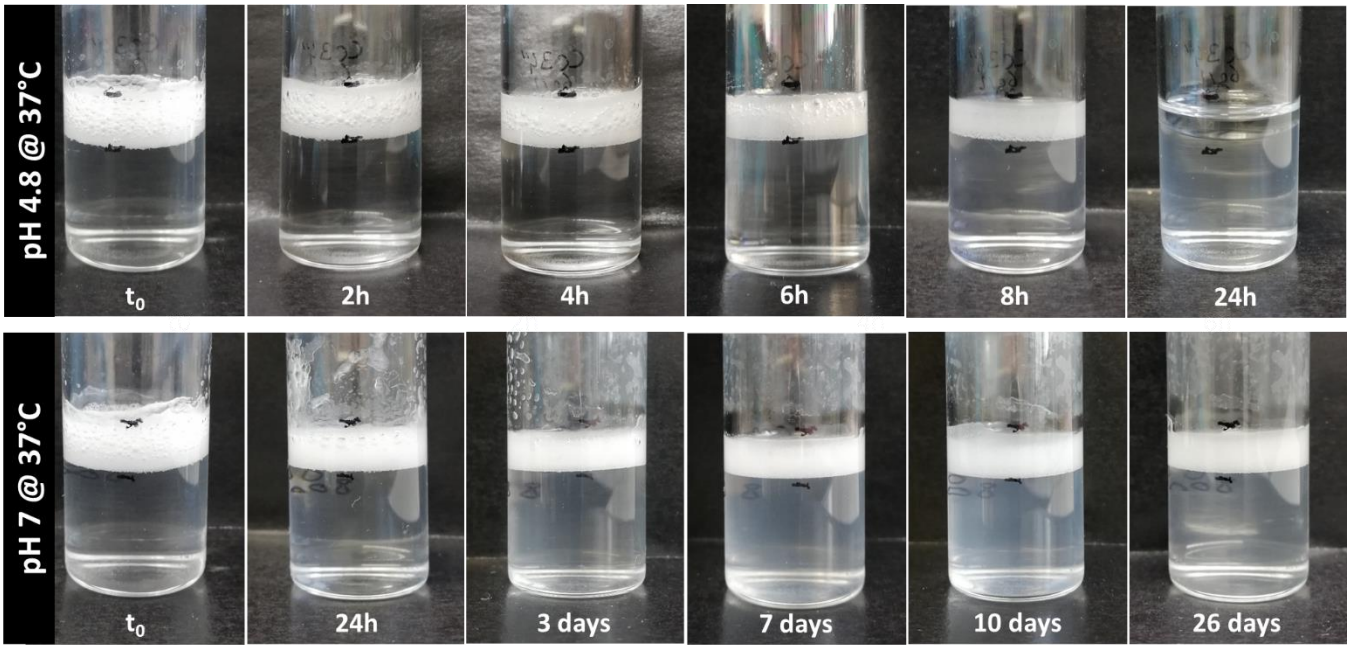

Figure 8. Macroscopic aspects of the formulated emulsions over time – with acidic buffer at pH 4.8 (top) and only with water at pH 7 (bottom) as a control.

Total emulsion destabilization at pH 4.8 after 24 h can clearly be seen on Figure 8. The emulsion cream level did not change a lot, but the cream opacity did attest a size evolution. As the number of droplets (submitted to coalescence as showed before) decreased, it minimized the multiple light scattering which is responsible for the white color of the cream. After 8 h, the emulsion remained stable whereas nanoparticles were fully hydrolyzed after 6 h under the same acidic conditions. This can be due to the lower available surface area when nanoparticles are anchored at the oil/water interface. However, the continuous phase seemed a little bit bluish after 8 h (and 24 h). It means that some nanoparticles were desorbed from the interface, which is in accordance with microscopic observations. The subnatant became completely transparent after few days confirming the total dissolution of the already desorbed nanoparticles. Th control sample did not show any major changes over a month, except air bubbles expelling.

From this two-scale study, it can be concluded that this Pickering emulsion system is fully demixed in 24 h under acidic conditions and most of all, there is no particle residue in the water medium.

3.5. Transferability of the system to other oils

The adsorption energy of a particle at an oil/water interface is directly proportional to the tension of the oil-water interface. It means that for high values, the energy can be so huge that even a change in affinity would not allow the particle to desorb, this has been observed and explained in a recent published paper dealing also with pH-sensitive Pickering emulsions [14]. Thus, we can assume that our system would be easily transferable among a large range of water/oil systems as the destabilization mechanism relies on the degradation of the stabilizer itself and also because tension of the dodecane-water interface is one of the highest (γ = 52.55 $mN.m^{-1}$ at 25°C [36]).

All the previous studies have been performed using dodecane, a model oil for emulsion science to offer a proof of concept for this new Pickering emulsion system. However, still in the aim of pushing forward efforts for more sustainability, we wished to work with a biocompatible oil extensively used in the field of pharmaceutics: medium-chain triglyceride (MCT). This kind of oil is much more polar than dodecane and with a higher density (close to the density of water). Nanoparticles from NPD1 were used to formulate Pickering emulsions with MCT. The obtained emulsions are of the O/W type (for a 50/50 v/v and for a 80/20 v/v of water and oil).

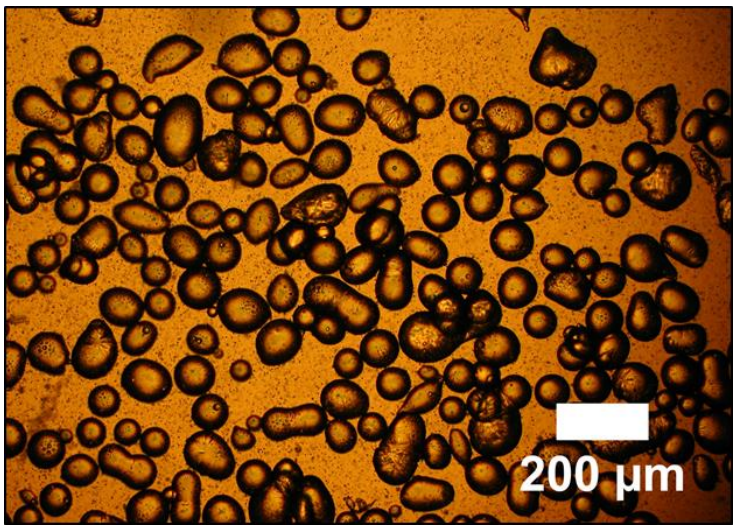

Figure 9. Microscopic structure of the MCT-in-water Pickering emulsion with a concentration of nanoparticles of 6 mg/mL of oil

Emulsion creaming took more time with MCT emulsions (compared to dodecane emulsions) as their density is closer to the one of water. Shape retention of droplets which started to coalesce can be seen in Figure 9. This phenomenon is typical of Pickering emulsions because interfaces are solid. Dodecane droplets were more spherical, the difference may come from the viscosity difference between the two oils. With a concentration of nanoparticles of 6 mg/mL, the measured D[3,2] was equal to 74 ± 15 µm (more difficult to define because of non-spherical drops). At the same concentration, D[3,2] of dodecane droplets was equal to 90 ± 19 µm which is pretty close.

Despite their higher polarity, MCT emulsions were kinetically stable over more than 3 weeks at room temperature. It means that both apolar and polar oil droplets could be stabilized by Ace-dextran NPs. Turbid aspect of the subnatants may come from very tiny droplets which did not cream, again because of the higher oil density. However, this population represent an insignificant volume compared to the whole volume of the dispersed phase. Using the same conditions as before, MCT emulsion stabilized by nanoparticles from NPD1 (6 mg / mL oil) was subjected to pH-induced destabilization by injection of an acetic buffer at pH 4.8 (Figure 10). A quicker destabilization (compared to dodecane) seemed

to appear 8 h after injection and in less than 24 h, the emulsion is fully demixed. The control sample showed no destabilization clue after 5 days.

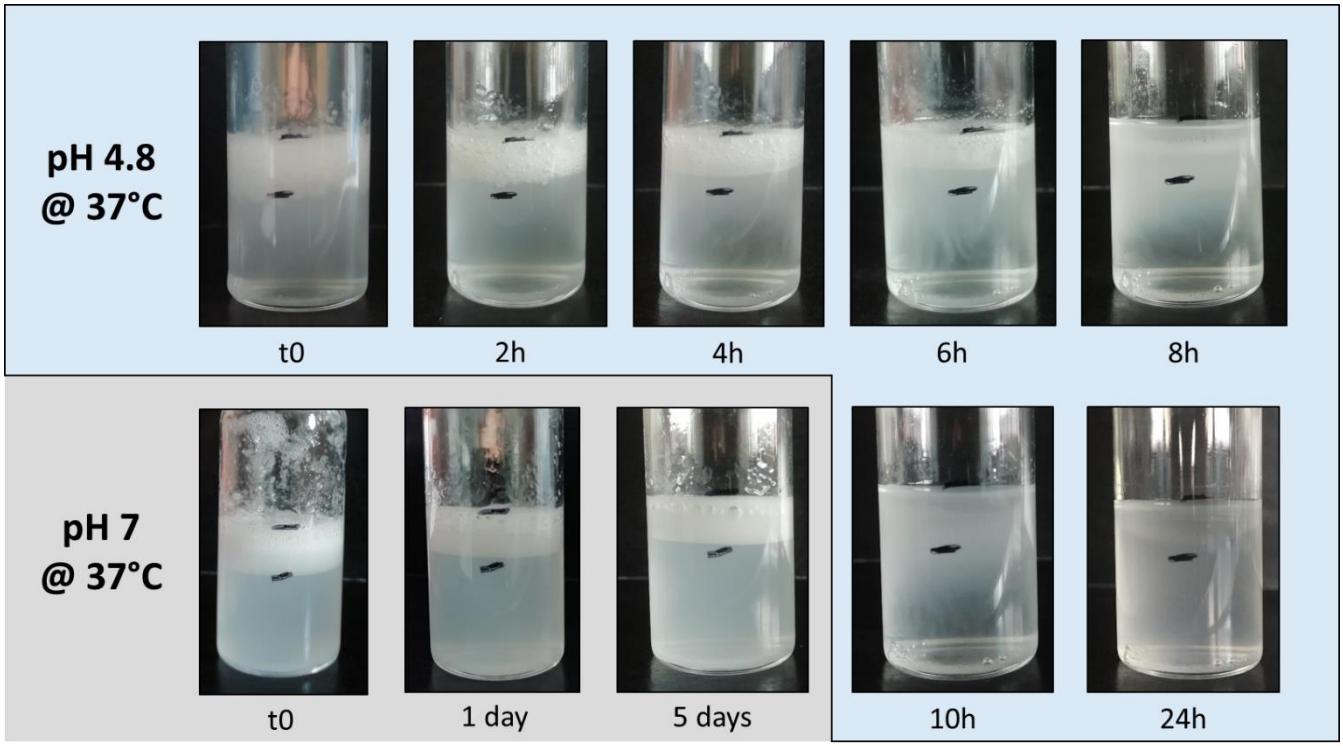

Figure 10: Macroscopic aspects of the MCT emulsions over time – with acidic buffer at pH 4.8 (blue area) and with only water at pH 7 (gray area)

This experiment show that the proposed strategy can be generalized. We are therefore convinced that this system will draw attention from both academic and industrial sides because it is fully bio-sourced, biocompatible and biodegradable.

4. Conclusions

In summary, we modified dextran (a biosourced, biocompatible, and biodegradable polysaccharide) to make it more hydrophobic and pH sensitive. Using nanoprecipitation, we were able to produce for the first time narrow-sized nanoparticles of pure Ace-dextran with a diameter around 200 nm and an average polymer density of 0.685 g/mL determined by MALS. They were then used to formulate stable Pickering emulsions which exhibited the typical limited coalescence phenomenon. This made it possible to produce in a repeatable way, size-controlled and narrow monomodal Pickering emulsions. Nanoparticles of Ace-dextran are degradable under acidic conditions and this hydrolysis yields acetone, ethanol and dextran, three biocompatible and simple (macro)molecules. The Pickering emulsions can be then destabilized by the addition of an acidic buffer, leading to a total system degradation within less than 24 hours. BecauseAce-dextran from a 50 min-long synthesis was used, by decreasing (or increasing) this reaction duration one can expect to decrease the time needed to hydrolyze the nanoparticles (or increase respectively) [22]. This will be of great importance because it means that we can also tune the emulsion degradation time (and for instance the release of active compounds). Pickering emulsions of biocompatible oil MCT were also formulated to obtain a pH-sensitive and totally green system which may be of high interest for biomedical and cosmetics applications. Moreover, catalysis or engineering of original materials [37] can be also considered. We are convinced that this new kind of carrier – and a new Pickering emulsion stabilizer class - will attract much interest, as it comprises biomass recovery, tunability and induced degradability.

CRediT authorship contribution statement

V. Maingret: Conceptualization, Investigation, Writing - original draft. **C. Courrégelongue:** Investigation, Writing - original draft. **V. Schmitt:** Conceptualization, Writing - review & editing, Supervision. **V. Héroguez:** Conceptualization, Writing - review & editing, Supervision.

Acknowledgments

V. M. acknowledges support from the Ministère de l'Enseignement Supérieur, de la Recherche et de l'Innovation for his Ph.D. grant. The authors thank their respective academic institution for financial support. The authors also acknowledge Paul Marque and Christophe Schatz for their help in MALS measurements analysis and Isabelle Ly for Cryo-SEM observations.

Supporting information

^{1}H NMR of Ace-dextran from S1 and S2 and calculations, multi-angle SLS methods calculations and results, DCR calibration curve using NPD2, stacked size distribution curves of NPD1 at t_0 and $t_{10months}$, and size measurements of Pickering emulsions stabilized by NPD1 nanoparticles.

References

(1) Wu, J.; Ma, G. H. Recent Studies of Pickering Emulsions: Particles Make the Difference. *Small* **2016**, *12* (34), 4633–4648. https://doi.org/10.1002/smll.201600877.

(2) Ramsden, W. Separation of Solids in the Surface-Layers of Solutions and 'Suspensions' (Observations on Surface-Membranes, Bubbles, Emulsions, and Mechanical Coagulation).—Preliminary Account. *Proc. Roy. Soc.* **1903**, *72*, 156–164.

(3) Pickering, S. U. CXCVI.—Emulsions. *J. Chem. Soc., Trans.* **1907**, *91*, 2001–2021. https://doi.org/10.1039/CT9079102001.

(4) Binks, B. P. Particles as Surfactants—Similarities and Differences. *Curr. Opin. Colloid Interface Sci.* **2002**, *7* (1–2), 21–41. https://doi.org/10.1016/S1359-0294(02)00008-0.

(5) Tang, J.; Quinlan, P. J.; Tam, K. C. Stimuli-Responsive Pickering Emulsions: Recent Advances and Potential Applications. *Soft Matter* **2015**, *11* (18), 3512–3529. https://doi.org/10.1039/c5sm00247h.

(6) Piao, S. H.; Kwon, S. H.; Zhang, W. L.; Choi, H. J. Celebrating Soft Matter's 10th Anniversary: Stimuli-Responsive Pickering Emulsion Polymerized Smart Fluids. *Soft Matter* **2015**, *11* (4), 646–654. https://doi.org/10.1039/c4sm02393e.

(7) Harman, C. L. G.; Patel, M. A.; Guldin, S.; Davies, G. L. Recent Developments in Pickering Emulsions for Biomedical Applications. *Curr. Opin. Colloid Interface Sci.* **2019**, *39*, 173–189. https://doi.org/10.1016/j.cocis.2019.01.017.

(8) Mwangi, W. W.; Lim, H. P.; Low, L. E.; Tey, B. T.; Chan, E. S. Food-Grade Pickering Emulsions for Encapsulation and Delivery of Bioactives. *Trends Food Sci. Technol.* **2020**, *100* (March), 320–332. https://doi.org/10.1016/j.tifs.2020.04.020.

(9) Tatry, M. C.; Qiu, Y.; Lapeyre, V.; Garrigue, P.; Schmitt, V.; Ravaine, V. Sugar-Responsive Pickering Emulsions Mediated by Switching Hydrophobicity in Microgels. *J. Colloid Interface Sci.* **2020**, *561*, 481–493. https://doi.org/10.1016/j.jcis.2019.11.023.

(10) Zhao, X.; Fang, X.; Yang, S.; Zhang, S.; Yu, G.; Liu, Y.; Zhou, Y.; Feng, Y.; Li, J. Light-Tuning Amphiphility of Host-Guest Alginate-Based Supramolecular Assemblies for Photo-Responsive Pickering Emulsions. *Carbohydr. Polym.* **2021**, *251* (June 2020), 117072. https://doi.org/10.1016/j.carbpol.2020.117072.
(11) Xie, C. Y.; Meng, S. X.; Xue, L. H.; Bai, R. X.; Yang, X.; Wang, Y.; Qiu, Z. P.; Binks, B. P.; Guo, T.; Meng, T. Light and Magnetic Dual-Responsive Pickering Emulsion Micro-Reactors. *Langmuir* **2017**, *33* (49), 14139–14148. https://doi.org/10.1021/acs.langmuir.7b03642.
(12) Hao, Y.; Liu, Y.; Yang, R.; Zhang, X.; Liu, J.; Yang, H. A PH-Responsive TiO_2-Based Pickering Emulsion System for in Situ Catalyst Recycling. *Chinese Chem. Lett.* **2018**, *29* (6), 778–782. https://doi.org/10.1016/j.cclet.2018.01.010.
(13) Low, L. E.; Ooi, C. W.; Chan, E. S.; Ong, B. H.; Tey, B. T. Dual (Magnetic and pH) Stimuli-Reversible Pickering Emulsions Based on Poly(2-(Dimethylamino)Ethyl Methacrylate)-Bonded Fe_3O_4 Nanocomposites for Oil Recovery Application. *J. Environ. Chem. Eng.* **2020**, *8* (2), 103715. https://doi.org/10.1016/j.jece.2020.103715.
(14) Qi, L.; Luo, Z.; Lu, X. Facile Synthesis of Starch-Based Nanoparticle Stabilized Pickering Emulsion: Its pH-Responsive Behavior and Application for Recyclable Catalysis. *Green Chem.* **2018**, *20* (7), 1538–1550. https://doi.org/10.1039/c8gc00143j.
(15) Li, W.; Ju, B.; Zhang, S. Novel Amphiphilic Cellulose Nanocrystals for pH-Responsive Pickering Emulsions. *Carbohydr. Polym.* **2020**, *229* (October 2019), 115401. https://doi.org/10.1016/j.carbpol.2019.115401.
(16) Zoppe, J. O.; Venditti, R. A.; Rojas, O. J. Pickering Emulsions Stabilized by Cellulose Nanocrystals Grafted with Thermo-Responsive Polymer Brushes. *J. Colloid Interface Sci.* **2012**, *369* (1), 202–209. https://doi.org/10.1016/j.jcis.2011.12.011.
(17) Glasing, J.; Jessop, P. G.; Champagne, P.; Cunningham, M. F. Graft-Modified Cellulose Nanocrystals as CO_2-Switchable Pickering Emulsifiers. *Polym. Chem.* **2018**, *9* (28), 3864–3872. https://doi.org/10.1039/c8py00417j.
(18) Liu, H.; Wang, C.; Zou, S.; Wei, Z.; Tong, Z. Simple, Reversible Emulsion System Switched by pH on the Basis of Chitosan without Any Hydrophobic Modification. *Langmuir* **2012**, *28* (30), 11017–11024. https://doi.org/10.1021/la3021113.
(19) Ren, D.; Xu, S.; Sun, D.; Wang, Q.; Xu, Z. CO_2-Switchable Dispersion of a Natural Chitosan and Its Application as a Responsive Pickering Emulsifier. *Colloids Surfaces A Physicochem. Eng. Asp.* **2018**, *555* (May), 507–514. https://doi.org/10.1016/j.colsurfa.2018.06.068.
(20) Baldwin, A. D.; Kiick, K. L. Polysaccharide-Modified Synthetic Polymeric Biomaterials. *Biopolymers* **2010**, *94* (1), 128–140. https://doi.org/10.1002/bip.21334.
(21) Moosavi-nasab, M.; Gavahian, M.; Yousefi, A. R.; Askari, H.; Culture, A. S. Fermentative Production of Dextran Using Food Industry Wastes. *World Acad. Sci. Eng. Technol.* **2010**, *44* (8), 1043–1045.
(22) Kauffman, K. J.; Do, C.; Sharma, S.; Gallovic, M. D.; Bachelder, E. M.; Ainslie, K. M. Synthesis and Characterization of Acetalated Dextran Polymer and Microparticles with Ethanol as a Degradation Product. *ACS Appl. Mater. Interfaces* **2012**, *4* (8), 4149–4155. https://doi.org/10.1021/am3008888.
(23) Arditty, S.; Whitby, C. P.; Binks, B. P.; Schmitt, V.; Leal-Calderon, F. Some General Features of Limited Coalescence in Solid-Stabilized Emulsions. *Eur. Phys. J. E* **2003**, *11* (3), 273–281. https://doi.org/10.1140/epje/i2003-10018-6.
(24) Araiza-Calahorra, A.; Glover, Z. J.; Akhtar, M.; Sarkar, A. Conjugate Microgel-Stabilized Pickering Emulsions: Role in Delaying Gastric Digestion. *Food Hydrocoll.* **2020**, *105* (February), 105794. https://doi.org/10.1016/j.foodhyd.2020.105794.
(25) Bachelder, E. M.; Beaudette, T. T.; Broaders, K. E.; Dashe, J.; Fréchet, J. M. J. Acetal-Derivatized Dextran: An Acid-Responsive Biodegradable Material for Therapeutic Applications. *J. Am. Chem. Soc.* **2008**, *130* (32), 10494–10495. https://doi.org/10.1021/ja803947s.
(26) Pang, S. C.; Chin, S. F.; Tay, S. H.; Tchong, F. M. Starch-Maleate-Polyvinyl Alcohol

Hydrogels with Controllable Swelling Behaviors. *Carbohydr. Polym.* **2011**, *84* (1), 424–429. https://doi.org/10.1016/j.carbpol.2010.12.002.
(27) Shang, J.; Gao, X. Nanoparticle Counting: Towards Accurate Determination of the Molar Concentration. *Chem. Soc. Rev.* **2014**, *43* (21), 7267–7278. https://doi.org/10.1039/c4cs00128a.
(28) Luque-Alcaraz, A. G.; Lizardi-Mendoza, J.; Goycoolea, F. M.; Higuera-Ciapara, I.; Argüelles-Monal, W. Preparation of Chitosan Nanoparticles by Nanoprecipitation and Their Ability as a Drug Nanocarrier. *RSC Adv.* **2016**, *6* (64), 59250–59256. https://doi.org/10.1039/c6ra06563e.
(29) Tarhini, M.; Benlyamani, I.; Hamdani, S.; Agusti, G.; Fessi, H.; Greige-Gerges, H.; Bentaher, A.; Elaissari, A. Protein-Based Nanoparticle Preparation via Nanoprecipitation Method. *Materials (Basel).* **2018**, *11* (3), 1–18. https://doi.org/10.3390/ma11030394.
(30) Soliman, S. M. A.; El Founi, M.; Vanderesse, R.; Acherar, S.; Ferji, K.; Babin, J.; Six, J. L. Light-Sensitive Dextran-Covered PNBA Nanoparticles to Continuously or Discontinuously Improve the Drug Release. *Colloids Surf., B* **2019**, *182* (May), 110393. https://doi.org/10.1016/j.colsurfb.2019.110393.
(31) Gavory, C.; Durand, A.; Six, J. L.; Nouvel, C.; Marie, E.; Leonard, M. Polysaccharide-Covered Nanoparticles Prepared by Nanoprecipitation. *Carbohydr. Polym.* **2011**, *84* (1), 133–140. https://doi.org/10.1016/j.carbpol.2010.11.012.
(32) Shkodra-Pula, B.; Kretzer, C.; Jordan, P. M.; Klemm, P.; Koeberle, A.; Pretzel, D.; Banoglu, E.; Lorkowski, S.; Wallert, M.; Höppener, S.; Stumpf, S.; Vollrath, A.; Schubert, S.; Werz, O.; Schubert, U. S. Encapsulation of the Dual FLAP/MPEGS-1 Inhibitor BRP-187 into Acetalated Dextran and PLGA Nanoparticles Improves Its Cellular Bioactivity. *J. Nanobiotechnology* **2020**, *18* (1), 1–14. https://doi.org/10.1186/s12951-020-00620-7.
(33) Whitesides, T. H.; Ross, D. S. Experimental and Theoretical Analysis of the Limited Coalescence Process: Stepwise Limited Coalescence. *J. Colloid Interface Sci*. 1995, pp 48–59. https://doi.org/10.1006/jcis.1995.1005.
(34) Schmitt, V.; Destribats, M.; Backov, R. Colloidal Particles as Liquid Dispersion Stabilizer: Pickering Emulsions and Materials Thereof. *Comptes Rendus Phys.* **2014**, *15* (8–9), 761–774. https://doi.org/10.1016/j.crhy.2014.09.010.
(35) Destribats, M.; Gineste, S.; Laurichesse, E.; Tanner, H.; Leal-Calderon, F.; Héroguez, V.; Schmitt, V. Pickering Emulsions: What Are the Main Parameters Determining the Emulsion Type and Interfacial Properties? *Langmuir* **2014**, *30* (31), 9313–9326. https://doi.org/10.1021/la501299u.
(36) Zeppieri, S.; Rodríguez, J.; López De Ramos, A. L. Interfacial Tension of Alkane + Water Systems. *J. Chem. Eng. Data* **2001**, *46* (5), 1086–1088. https://doi.org/10.1021/je000245r.
(37) Xu, Y.; Ge, X.; Ji, X.; Wang, M.; Ge, X. Synthesis of Golf-Ball-like Polystyrene Microspheres from a Pickering Emulsion Stabilized by Amphiphilic Janus Microspheres. *Chem. Lett.* **2013**, *42* (9), 963–965. https://doi.org/10.1246/cl.130297.

Table of Contents graphic